J|A|C|S COMMUNICATIONS

Published on Web 01/28/2010

Polymorphism and Reversible Mechanochromic Luminescence for Solid-State Difluoroboron Avobenzone

Guoqing Zhang,[†] Jiwei Lu,[‡] Michal Sabat,[†] and Cassandra L. Fraser*[,†]

Department of Chemistry and Department of Materials Science and Engineering, University of Virginia, Charlottesville, Virginia 22904

Received November 17, 2009; E-mail: fraser@virginia.edu

The solid-state fluorescence of organic molecules strongly depends on the molecular structure and intermolecular interactions present in different morphologies.[1] Various emission colors[2−4] may be achieved from the same fluorophore by taking advantage of material polymorphism, which is controllable by processing methods.[5] Another more unusual strategy involves force-induced emission color changes, or mechanochromic luminescence.[6,7] For some mechanoresponsive gold complexes,[8,9] the photoluminescence can be switched by grinding. For example, ordered aggregates and an amorphous solid are responsible for the blue and yellow emission colors, respectively, of $[(C_6F_5Au)_2(\mu$-1,4-diisocyanobenzene)].[10] Mechanochromic luminescence has also been attributed to the disruption of hydrogen bonding,[11] resulting in a less ordered polymorph. More recently, Chung et al.[12] reported fluorescence "turn on" by either UV irradiation or shear force for a cyanostilbene system. Though compelling hypotheses have been advanced for all of these systems, a molecular-level understanding of the mechanochromic mechanisms remains unclear. Furthermore, in all of these examples, the initial and mechanically perturbed states of the materials are stable and readily characterized. The perturbed states must be treated with solvent or heat to revert back to the initial state. Here we report that solid-state difluoroboron avobenzone (BF_2AVB; Figure 1) possesses unexpected narrow-band, morphology-dependent fluorescence. It also exhibits unusual reversible mechanochromic fluorescence that recovers spontaneously at room temperature or more quickly with heating.

Avobenzone (AVB) is a commercially available substance used as an ingredient in sunscreen products because of its strong absorption of UVA light (320−400 nm).[13] It is also easily prepared by Claisen condensation of 4-methoxyacetophenone and methyl 4-*tert*-butylbenzoate. The difluoroboron complex BF_2AVB was synthesized via $BF_3{\cdot}OEt_2$ boronation in CH_2Cl_2. The optical properties were first investigated in CH_2Cl_2 solution. The absorption (λ_{max} = 402 nm), fluorescence emission (λ_{em} = 433 nm), high quantum yield (Φ_F = 0.90), and lifetime (single-exponential, τ_F = 1.9 ns) are typical for dyes of this type.[14,15] During slow solvent evaporation, BF_2AVB forms two different types of crystals: large, green-emitting prismlike crystals and cyan-emitting needlelike crystals. Images of BF_2AVB crystals under UV excitation are shown in Figure 1. While exploring different processing conditions, we discovered another very interesting solid-state form (Figure 1D) via CH_2Cl_2 evaporation from a cotton swab. The morphology of the material thus fabricated was examined using scanning electron microscopy (SEM), which revealed dendritic BF_2AVB solids typically several hundred micrometers in size with highly porous surfaces consisting of feathery thin sheets (Figure 1E,F).

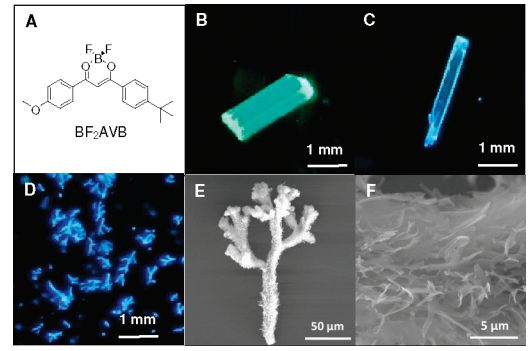

Figure 1. (A) Chemical structure of BF_2AVB. (B−D) Photos showing (B) green and (C) cyan crystals and (D) the blue coral-like solid under UV excitation (λ_{ex} = 365 nm). (E) SEM image of the dendritic coral-like structure. (F) Magnified view of the porous surface.

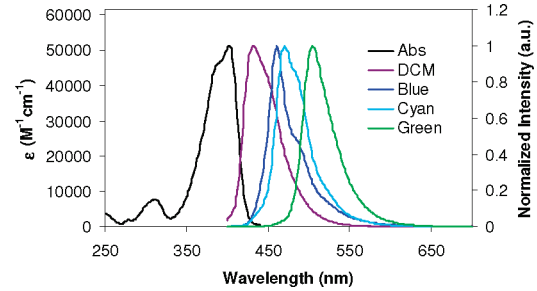

Figure 2. Absorption spectrum in CH_2Cl_2 (DCM) (black trace) and fluorescence emission spectra (λ_{ex} = 369 nm) for BF_2AVB in optically dilute CH_2Cl_2 solution (violet) and as dendritic (blue), needle (cyan), and prism (green) solids (fwhm = 47, 31, 42, and 41 nm, respectively).

Under a UV lamp, the prism, needle, and dendritic solid forms of BF_2AVB exhibit green, cyan, and blue emissions, respectively. Steady-state fluorescence spectra are shown in Figure 2. Normally, $BF_2(\beta$-diketonate$)_{(s)}$ emission is significantly red-shifted and broadened relative to dye solutions.[16] For example, many difluoroboron dibenzoylmethane (dbm) derivatives show bathochromic shifts of ∼100 nm with ∼50 nm band width broadening.[17] In contrast, all three BF_2AVB solids show very narrow band width emission relative to fluorescence in CH_2Cl_2 [λ_{em} = 433 nm; full width at half-maximum (fwhm) = 47 nm]. Among them, the dendritic solid formed by rapid solvent evaporation shows the most narrow emission band (fwhm = 31 nm), with peak intensity at λ_{max} = 459 nm. The emission spectra are surprisingly reproducible by this simple method (Figure S1 in the Supporting Information). The cyan- and green-emitting crystals have emission maxima at 470 and 505 nm and fwhm values of 42 and 41 nm, respectively. Notably, the dendritic solid has a rich emission structure, perhaps due to vibrational or multicomponent contributions. The fluorescence

[†] Department of Chemistry.
[‡] Department of Materials Science and Engineering.

10.1021/ja9097719

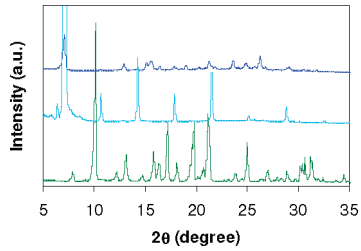

Figure 3. XRD patterns for the (top) blue solid, (middle) cyan crystal, and (bottom) green crystal forms of BF_2AVB.

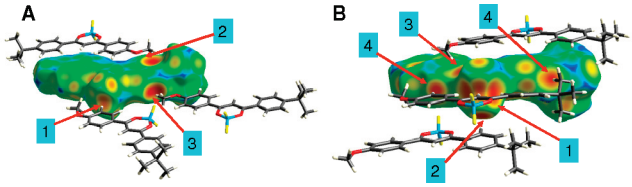

Figure 4. Crystal packing for (A) green and (B) cyan BF_2AVB crystals, showing Hirshfeld surfaces of the central molecules mapped with d_e. The most significant intermolecular interactions are: (A1) C(arene)−H···F hydrogen bond; (A2) C(methyl)−H···π interaction; (A3) short H···H contacts; (B1, B2) C(arene)−H···F hydrogen bonds; (B3) C(methyl)−H···O hydrogen bond; (B4) short H···H contacts.

lifetimes of the green, cyan, and blue solids exhibit a decreasing trend of 16.7, 6.9, and 5.4 ns. Also, both of the single crystals show single-exponential decay (Figures S2 and S3). The dendritic solid can be fit to double-exponential decay (Figure S4), where a more heterogeneous molecular environment may be present than in the single crystals.

X-ray diffraction (XRD) patterns show distinctly different structures for the three BF_2AVB solid forms (Figure 3). Single-crystal X-ray analysis was also performed for BF_2AVB crystals (Figure S5). In the green crystal, the boron diketone and phenyl rings are coplanar, whereas the *tert*-butyl aromatic ring in the cyan crystal is twisted ∼8° relative to the BF_2 diketone arene plane (Figure S6). Furthermore, the crystal lattices of the two forms have different symmetries. In the green crystal, the molecules are antiparallel (*tert*-butyl groups on opposite sides) with the arenes offset relative to each other in the stacked dimer (i.e., both dioxaborine rings are paired with PhOMe rings). In the cyan system, in contrast, the *tert*-butyl groups are clustered on the same side of the dimers, which bear both a dioxaborine−PhOMe and a dioxaborine−Ph-*t*-Bu stacked pair. The shorter conjugation length in the twisted structure and weaker $\pi-\pi$ stacking may help to explain the relatively blue-shifted emission for the cyan crystal versus the green one.

Hirshfeld surface calculations[18] provide additional insight into the molecular interactions in the BF_2AVB structures. Distances to the nearest atoms outside (intermolecular, d_e) and inside (intramolecular, d_i) are used for color-coded mapping of the surface (red, closest contacts; blue, very little or no interaction). The twisted conformation in the cyan crystal corresponds to stronger intermolecular interactions, as illustrated in the d_e-mapped Hirshfeld surfaces in Figure 4. The molecular surfaces (Figures S7 and S8) and relevant fingerprint plots (Figure S9) suggest closer C(methyl)−H···O and C(arene)−H···F contacts (including possible C−H···F hydrogen bonds) in the cyan form than in the green form.

The morphology-sensitive solid-state emission of BF_2AVB was also evident upon mechanical perturbation. When the blue-emitting BF_2AVB dendritic solid (∼3 mg) was smeared onto a piece of weighing paper (2 × 2 in^2), it exhibited yellow emission under UV blacklight excitation (λ_{ex} = 365 nm). After a few minutes, the

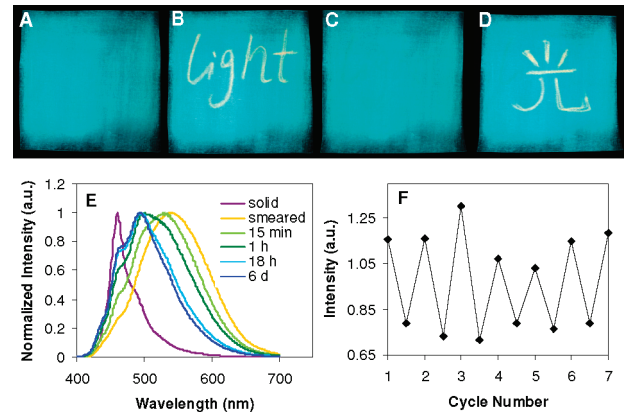

Figure 5. (A) Fluorescence emission (λ_{ex} = 365 nm) of a thermally annealed BF_2AVB solid film on a piece of weighing paper. (B) Mechanochromic fluorescence of "light" written with a cotton swab tip. (C) Background emission restored by heating the film with a heat gun for ∼3−5 s. (D) Rewritable mechanochromic fluorescence demonstrated by the Chinese character "light" generated with a cotton swab tip. (E) Fluorescence emission spectra of the BF_2AVB blue solid and the smeared solid film on a quartz substrate monitored over time after smearing. (F) Fluorescence emission intensity monitored at 535 nm vs smearing/thermal erasing cycle number.

bright yellow fluorescence faded, and a greenish emission emerged. This fading process was facilitated by brief heating (∼30 s in an ∼110 °C oven or ∼3−5 s with a heat gun), resulting in a green-blue emission color under UV excitation. After the material was thermally annealed, even a small mechanical perturbation, such as a slight touch with the tip of a cotton swab, changed the green-blue BF_2AVB film emission to yellow (Figure 5). The yellow emission gradually reverted back to green again at room temperature, with much faster recovery at elevated temperature. The written regions were no longer readable after annealing.

Mechanochromic emission changes for solid-state BF_2AVB were also investigated by fluorescence spectroscopy. Figure 5E shows the initial and postsmearing fluorescence spectra for the solid on a quartz substrate as a function of recovery time. Consistent with visual observation, after BF_2AVB was smeared, the fluorescence spectrum was drastically broadened, with the fwhm increasing from 30 to 119 nm. The corresponding emission maximum shifted from 460 to 542 nm with a tiny shoulder at ∼460 nm, which closely matches the starting solid emission. The recovery dynamics are also evident from the spectra recorded at different times. After the film was smeared, the blue shoulder grew (up to 1 h), the main peak gradually blue-shifted, and the fwhm decreased with time. The emission color stabilized after ∼1 day and could be switched back to yellow emission with smearing. Regardless of the initial state (single crystal or dendritic solid), smeared BF_2AVB solids exhibit similar yellow emission, and their recovery dynamics are also similar as long as the smeared solid films have approximately the same thickness. (Slower recovery was observed for thicker films.) Figure 5F verifies the fluorescence "rewritability" of a BF_2AVB solid film on a piece of weighing paper.

Both Ito et al.[10] and Sagara et al.[11] have reported that red-shifted emissions in mechanochromic luminescent materials are related to the amorphous state and that the crystalline state is responsible for the blue emissions. Their claims have been supported by XRD experiments. It is not clear, however, in the case of solid-state BF_2AVB what specific interactions are responsible for the strong tendency for molecular organization after smearing, even at temperatures much lower than the melting point (234−236 °C). The strong dipolar[19] nature of BF_2dbm derivatives, offset arene stacking, hydrogen bonding between the fluorine and arene H

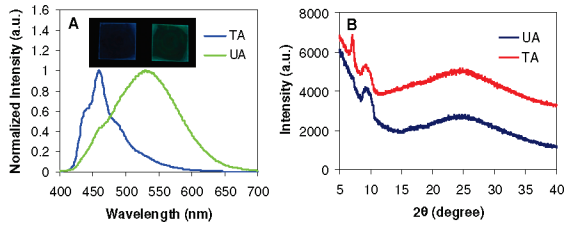

Figure 6. Photos (A inset) showing the BF_2AVB spin-cast films under UV excitation and their corresponding (A) emission spectra and (B) XRD patterns for unannealed (UA) and thermally annealed (TA) samples.

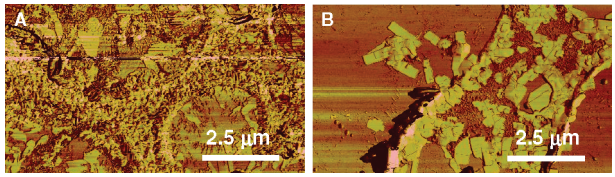

Figure 7. AFM images of BF_2AVB spin-cast films on glass substrates (A) before and (B) after thermal annealing.

atoms,[20,21] and other interactions could be involved. After green BF_2AVB crystals were thoroughly ground, there were no major differences in the XRD patterns; only very minor peak shifts (<0.5°) and relative intensity changes were observed (Figure S10).

We also attempted to create a more stable amorphous BF_2AVB film on a glass substrate by spin-coating from CH_2Cl_2 solution. The emission spectrum of the resulting film resembles that of the smeared BF_2AVB solid. It is significantly red-shifted and broadened (λ_F = 530 nm, τ = 24.7 ns) (Figure 6A). Thermal annealing at 110 °C for 5 min, however, turned the film emission blue (λ_F = 459 nm, τ = 3.87 ns). BF_2AVB film microstructures before and after thermal treatment were examined with XRD and atomic force microscopy (AFM). Figure 6B shows a sharp peak at $2\theta = 5.3°$ only for the heat-treated film, suggestive of a crystalline transformation during the annealing process. AFM images reveal well-defined rectangular sheetlike aggregates after thermal treatment (Figure 7). Some regions of the amorphous film appeared crystalline even before heating, suggesting a strong tendency for ordering.

Data suggest that the yellow emission may arise from the amorphous state of BF_2AVB, whereas excimers may form in mechanically perturbed regions as a result of greater rotational freedom.[6,22,23] Furthermore, excimers may serve as low-energy traps for exciton transfer in the crystals, which may help to explain the observed emission color changes and relative retention of XRD features. This hypothesis is also supported by fluorescence spectroscopy at 77 K, where the freshly smeared regions (which are yellow at room temperature) become green and the spectra match the background fluorescence of the unscratched annealed film. The yellow emission is restored in the scratched regions as the sample is warmed back to room temperature (Figure S11). If BF_2AVB excimer formation requires a conformational change, rigidifying the solid may suppress this process and efficiently reduce the yellow emission from the smeared regions. Finally, although the emission of the smeared region is red-shifted, its excitation spectrum is actually blue-shifted relative to that of the blue dendritic solid (Figure S12). This suggests that the yellow emission after smearing is due to an excited-state effect rather than ground-state association.

In summary, we have reported morphology-dependent fluorescence and unusual reversible mechanochromic luminescence for solid-state BF_2AVB. Unlike previously reported $BF_2dbm_{(s)}$ derivatives that typically exhibit strongly red-shifted and significantly broadened fluorescence spectra, $BF_2AVB_{(s)}$ shows unexpectedly sharp emission spectra that can be tuned via the solid form, such as single crystals, dendritic solid, or spin-cast film. Single-crystal XRD revealed that BF_2AVB molecules can form multiple emissive aggregation states with different intermolecular interactions. The fluorescence color is dramatically altered after crushing or physically smearing BF_2AVB crystals or upon scratching or rubbing annealed film samples. The mechanochromic fluorescence recovers reproducibly. From a material design standpoint, the fact that the scratched or rubbed region emission fades over time and merges with the background color makes BF_2AVB a self-healing optical material. The relationship between dye structure, solid-state emission color, and recovery time is under exploration.

Acknowledgment. We thank the National Science Foundation (CHE 0718879) for support of this work.

Supporting Information Available: Experimental methods, supporting figures, and crystallographic data (CIF). This material is available free of charge via the Internet at http://pubs.acs.org.

References

(1) Schwoerer, M.; Wolf, H. C. *Organic Molecular Solids*; Wiley-VCH: Weinheim, Germany, 2007.
(2) Mutai, T.; Satou, H.; Araki, K. *Nat. Mater.* **2005**, *4*, 685.
(3) Zhang, H.; Zhang, Z.; Ye, K.; Zhang, J.; Wang, Y. *Adv. Mater.* **2006**, *18*, 2369.
(4) Mizukami, S.; Houjou, H.; Sugaya, K.; Koyama, E.; Tokuhisa, H.; Sasaki, T.; Kanesato, M. *Chem. Mater.* **2005**, *17*, 50.
(5) Kohmoto, S.; Tsuyuki, R.; Masu, H.; Azumaya, I.; Kishikawa, K. *Tetrahedron Lett.* **2008**, *49*, 39.
(6) Sagara, Y.; Kato, T. *Angew. Chem., Int. Ed.* **2008**, *47*, 5175.
(7) Sagara, Y.; Kato, T. *Nat. Chem.* **2009**, *1*, 605.
(8) Lee, Y. A.; Eisenberg, R. *J. Am. Chem. Soc.* **2003**, *125*, 7778.
(9) Assefa, Z.; Omary, M. A.; McBurnett, B. G.; Mohamed, A. A.; Patterson, H. H.; Staples, R. J.; Fackler, J. P. *Inorg. Chem.* **2002**, *41*, 6274.
(10) Ito, H.; Saito, T.; Oshima, N.; Kitamura, N.; Ishizaka, S.; Hinatsu, Y.; Wakeshima, M.; Kato, M.; Tsuge, K.; Sawamura, M. *J. Am. Chem. Soc.* **2008**, *130*, 10044.
(11) Sagara, Y.; Mutai, T.; Yoshikawa, I.; Araki, K. *J. Am. Chem. Soc.* **2007**, *129*, 1520.
(12) Chung, J. W.; You, Y.; Huh, H. S.; An, B.-K.; Yoon, S.-J.; Kim, S. H.; Lee, S. W.; Park, S. Y. *J. Am. Chem. Soc.* **2009**, *131*, 8163.
(13) Chatelain, E.; Gabard, B. *Photochem. Photobiol.* **2001**, *74*, 401.
(14) Cogné-Laage, E.; Allemand, J.-F.; Ruel, O.; Baudin, J.-B.; Croquette, V.; Blanchard-Desce, M.; Jullien, L. *Chem.—Eur. J.* **2004**, *10*, 1445.
(15) Zhang, G.; Chen, J.; Payne, S. J.; Kooi, S. E.; Demas, J. N.; Fraser, C. L. *J. Am. Chem. Soc.* **2007**, *129*, 8942.
(16) Ono, K.; Yoshikawa, K.; Tsuji, Y.; Yamaguchi, H.; Uozumi, R.; Tomura, M.; Taga, K.; Saito, K. *Tetrahedron* **2007**, *63*, 9354.
(17) Mirochnik, A. G.; Bukvetskii, B. V.; Fedorenko, E. V.; Karasev, V. E. *Russ. Chem. Bull.* **2004**, *53*, 291.
(18) McKinnon, J. J.; Spackman, M. A.; Mitchell, A. S. *Acta Crystallogr., Sect. B* **2004**, *60*, 627.
(19) Brown, N. M. D.; Blandon, P. *J. Chem. Soc. A* **1969**, 526.
(20) Zhang, X.; Yan, C.-J.; Pan, G.-B.; Zhang, R.-Q.; Wan, L.-J. *J. Phys. Chem. C* **2007**, *111*, 13851.
(21) Rohde, D.; Yan, C.-J.; Wan, L.-J. *Langmuir* **2006**, *22*, 4750.
(22) Kozhevnikov, V.; Donnio, B.; Bruce, D. *Angew. Chem., Int. Ed.* **2008**, *47*, 6286.
(23) Abe, T.; Akura, T.; Ikeda, N.; Shinozaki, K. *Dalton Trans.* **2009**, 711.

JA9097719